Impact-parameter dependence of atomic Coulomb K-shell ionization cross sections in a peaked-binary-encounter approximation

J. H. McGuire
Department of Physics, Kansas State University, Manhattan, Kansas 66506
(Received 7 May 1973; revised manuscript received 30 July 1973)

Cross sections for the ionization of atoms by the impact of heavy, charged particles are expressed as a function of the impact parameter b of the incident projectile. The ionization probability $P(b)$, which is obtained in a peaked-binary-encounter approximation (BEA), is compared to several recent experiments and to the semiclassical Coulomb approximation (SCA). At high energies the BEA and plane-wave SCA models give the same result, the shape of which is proportional to a simple function of $2b/a$ (a is the atomic radius). The functional form is independent of both projectile and target for isotropic target-electron distributions. At low energies the BEA and SCA models give similar but not identical results. The scaling properties at low energies are the same for both models. Comparison to experimental results at intermediate energies does not strongly favor either model at this time. Typically, the shape of $P(b)$ is within $\sim 50\%$ of experiment. A table of $P(b)$ for the BEA model is given which, together with scaling laws, may be used to find $P(b)$ for arbitrary projectiles and targets at various energies.

I. INTRODUCTION

In principle, ion-atom scattering may be represented by a single quantum-mechanical wave function. In practice, however, such a wave function is often complicated both mathematically and conceptually. In the case of atomic ionization, where the projectile carries enough energy to excite an infinity of possible configurations, an exact understanding is practically impossible at the present time. Consequently, approximations and models have been introduced to provide a conceptual guide for the interpretation of experimental data.

The two models used most widely in interpreting data corresponding to total cross sections of atoms ionized by the impact of ions are the Born approximation[1] and the binary-encounter approximation[2] (BEA). It has been shown[3] that in the high-energy classical limit both approximations agree. Furthermore, both approximations are generally within 30–200% of experimental total ionization cross sections of atoms by proton and alpha-particle impact over a wide range of energies, including low energies, where application of these models is theoretically questionable. In other words, both of these models have served as a useful conceptual guide for quite a broad sampling of atomic total ionization cross sections.

Recently, there have been experimental studies[4-7] of the dependence of the ionization cross section on the impact parameter of the projectile, where it is assumed that the projectile may be localized as a classical particle, and that the projectile is deflected by Rutherford scattering with the target nucleus. In addition to being conceptually simple, these studies represent a finer probe of the ionization mechanism than do measurements of total cross sections. Moreover, they yield detailed information about the ionization probability as a function of the impact parameter. These studies of single scattering events may be used for multiple scattering where combinations of single scattering probabilities have been employed.

The underlying theoretical basis for these studies lies in time-dependent perturbation theory,[8] which defines the scattering amplitude as a function of impact parameter. In 1959 a detailed analysis of the ionization probability $P(b)$ was done in first-order time-dependent perturbation theory by Bang and Hansteen.[9] Such calculations,[10] now referred to as semiclassical Coulomb approximation (SCA) calculations, require the equivalent of at least four numerical integrations, in general, for the evaluation of $P(b)$ at each impact parameter and each value of the projectile energy. Recently, however, Brandt, Jones, and Kraner[6] have developed a simple algebraic expression for $P(b)$ which is within 1% of the SCA result for projectile velocities much less than the orbit velocity of the target electron.

In this paper, we develop an expression using the BEA model for $P(b)$ which requires a single numerical integration. Simple scaling laws are then derived for hydrogenic electrons. These scaling laws may be used, together with a table of $P(b)$ vs b over a wide energy range, to evaluate $P(b)$ for arbitrary projectiles and targets. Furthermore, the BEA scaling laws are the same as in the low-energy SCA approximation. At high energies it is shown that the BEA and SCA models give the same universal curve for $P(b)$. And

finally, a detailed comparison of the BEA and SCA results is made with recent experiments.

II. FORMULATION

A. Binary-Encounter Approximation

In the BEA calculation of total ionization cross sections, one first considers the Coulomb scattering of the incident projectile with velocity $\vec{v}_i$ with a free electron with velocity $\vec{v}_2$. In this system the energy transferred to the electron, ΔE, is a simple function of the scattering angle, and the differential scattering cross section is taken to be a function of ΔE. In order to compute cross sections for isotropically distributed atomic electrons, one then effectively integrates over the directions[11] of $\hat{v}_i$ and $\hat{v}_2$, and over energy transfers. All of this may be done in closed form, according to

$$\int^{\Delta E}\int d\Delta\, E\, d\hat{v}_i d\hat{v}_2 \frac{d\sigma}{d\Delta E}(\vec{v}_i, \vec{v}_2, \Delta E)\frac{|\vec{v}_i-\vec{v}_2|}{4\pi v_i} = \frac{z^2\pi e^4}{3v_i^2 v_2}\left(\frac{-2v_2^3}{(\Delta E)^2}-\frac{(6v_2/m)}{\Delta E}\right), \quad 0<\Delta E<b$$

$$= \frac{z^2\pi e^4}{3v_i^2 v_2}\left(3\,\frac{(v_i/M)-(v_2/m)}{\Delta E}+\frac{(v_2'^3-v_2^3)-(v_i'^3+v_i^3)}{(\Delta E)^2}\right), \quad b<\Delta E<a$$

$$= \frac{z^2\pi e^4}{3v_i^2 v_2}\left(\frac{-2v_i'^3}{(\Delta E)^2}\right), \quad \Delta E>a \text{ and } 2mv_2>(M-m)v_i$$

$$= 0, \quad \Delta E>a \text{ and } 2mv_2<(M-m)v_i, \text{ or if energy conservation is violated.} \tag{1}$$

Here M and m are the masses of the projectile and the electron, z is the projectile charge, and

$$\begin{aligned} a &= \frac{4Mm}{(M+m)^2}\left[E_i - E_2 + \tfrac{1}{2}v_i v_2 (M-m)\right], \\ b &= \frac{4Mm}{(M+m)^2}\left[E_i - E_2 - \tfrac{1}{2}v_i v_2 (M-m)\right], \\ v_i' &= (v_1^2 - 2\Delta E/M)^{1/2}, \quad v_2' = (v_2^2 + 2\Delta E/m)^{1/2}, \\ E_i &= \tfrac{1}{2}Mv_i^2, \quad E_2 = \tfrac{1}{2}mv_2^2. \end{aligned} \tag{2}$$

The cross section for removing a single atomic electron with binding energy $-U = \frac{1}{2}mv_0^2$ is then found by averaging over the density distribution of the atomic electron corresponding to

$$\sigma(V) = \int_0^\infty 4\pi v_2^2 \rho(v_2, v_0)\sigma_i(v_i, v_2)\, dv_2, \tag{3}$$

where $V = v_i/v_0$, and

$$\sigma_i = (v_i, v_2) \equiv \int_U^{E_i} d\Delta E \int d\hat{v}_i\, d\hat{v}_2 \frac{d\sigma}{d\Delta E} \times (\vec{v}_i, \vec{v}_2, \Delta E)\frac{|\vec{v}_i - \vec{v}_2|}{4\pi v_i}. \tag{4}$$

For hydrogenic electrons in closed shells, $\rho(v_2)$ is given by

$$\rho(v_2, v_0) = \frac{8}{\pi}\frac{v_0^5}{\pi(v_0^2+v_2^2)^4}, \tag{5}$$

and the total ionization cross section per target electron, corresponding to Eq. (3), may be simply expressed as

$$\sigma(V) = \frac{z^2\sigma_0}{U^2}G(V), \tag{6}$$

where $\sigma_0 = \pi e^4 = 6.56\times10^{-14}$ eV^2 cm^2, and $G(V)$ is a function of the scaled velocity $V = v_i/v_0$, which has been tabulated.[12]

B. Derivation of BEA $P(b)$

We now wish to express the BEA total ionization cross section per electron in the form

$$\sigma(V) = \int_0^R 2\pi b P(b)\, db, \tag{7}$$

corresponding to Fig. 1, where $P(b)$ is ionization probability per electron and R is the range of the interaction. First, we assume a relationship between $\vec{v}_2$ and $\vec{r}$ using conservation of energy, namely,

$$\tfrac{1}{2}mv_2^2 - \frac{Ze^2}{r} = |U| = \tfrac{1}{2}mv_0^2,$$

or

$$v_2(r) = (2a/r - 1)^{1/2}, \tag{8}$$

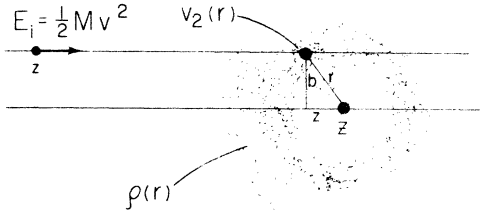

FIG. 1. Representation of the BEA Model. The incident projectile with velocity v_i scatters via a two-body Coulomb interaction from an electron with velocity v_2. The atomic electron is characterized by a density distribution $\rho(r)$.

where a is the orbital radius of the atomic electron.

Assuming that $\rho(\vec{v}_2(r))$ is isotropic in $\vec{v}_2$ at each $\vec{r}$, we rewrite Eqs. (3) and (4) as

$$\sigma(V)=\int_u^{E_i} d\Delta E \int dr\, 4\pi r^2 \rho(r) \int d\hat{v}_i\, d\hat{v}_2 \times \frac{d\sigma}{d\Delta E}(\vec{v}_i, \vec{v}_2, \Delta E)\frac{|\vec{v}_i, \vec{v}_2|}{4\pi v_i} \tag{9}$$

and consider a projectile with a well-defined impact parameter incident on an isotropic electron cloud, as depicted in Fig. 1. For an isotropic electron cloud there are only two directions defined by this problem—namely, $\hat{v}_i$ and $\hat{v}_2$. Since the cross section is a scalar quantity, the integration over $\hat{v}_i$ can depend only on v_i and v_2 (and not $\hat{v}_2$). Since v_2 depends on r (and not $\hat{r}$), we may directly use Eqs. (4) and (1) for $\sigma_i(v_i, v_2(r))$, and write

$$\sigma(V)=\int dr\, 4\pi r^2 \rho(r)\sigma(v_i, v_2(r)). \tag{10}$$

The integrand is an isotropic function of r, so that we may write

$$\sigma(V)=\int d^3r\, \rho(r)\sigma(v_i, v_2(r)) = \int_0^R db\, 2\pi b \int_{-(R^2-b^2)^{1/2}}^{+(R^2-b^2)^{1/2}} dz\, \rho((b^2+z^2)^{1/2}) \times \sigma(v_i, v_2[(b^2+z^2]^{1/2})),$$

where the integrand is zero for $r>R$. We now identify

$$P(b)=2\int_0^{(R^2-b^2)^{1/2}} \rho((b^2+z^2)^{1/2}) \times \sigma(v_i, v_2([b^2+z^2]^{1/2}))\, dz \tag{12}$$

as the ionization probability per electron. We now assume that the two-body cross section is peaked when the projectile and electron are close together, so that we may identify b as the impact parameter of the projectile. This approximation, introduced by Gryzinski,[13] is plausible for ionization since at large impact parameters the projectile cannot transfer enough energy to the electron to remove it from the atom. This idea may be expressed in a semiquantatative way by largely ignoring the target nucleus and writing $e^2/2a = U \leq \Delta E \leq (\Delta PE)_{\max} < ze^2/2\bar{b}$. As a result, $\bar{b} < za$, where b is the impact parameter of the projectile relative to the target electron.

It should be noted that this expression is not unique. Even a unique definition of $\vec{v}_2(\vec{r})$ and $\rho(r)$ would leave our expression for $P(b)$ formally non-unique, since equating two integrals does not necessarily equate the integrands.

At zero impact parameter, $P(0)$ may be expressed as

$$P(0)=\left\langle \frac{\sigma(v_i, v_2(r))}{2\pi r^2} \right\rangle, \tag{13}$$

corresponding to the average of twice the cross section for ionization divided by the surface area of the electron cloud. The factor of 2 indicates that the projectile has two chances of hitting the electron—namely, on the way in and on the way out.

In general, $P(b)$ is proportional to the density of the electron cloud seen by the projectile weighted by the cross section appropriate to $v_2(r)$. The total cross section $\sigma(V)$ is, of course, identical to that computed from Eq. (3).

C. Isotropic Hydrogenic Density Distributions

The density distribution corresponding to electrons in a hydrogenlike atomic K shell is not unique in our approximation. We could choose

$$\rho(r)=e^{-2r/a}/a^3 \quad [\, v_2(r)=0 \text{ for } r>2a\,] \tag{14}$$

corresponding to $|\psi(r)|^2$, or we could choose

$$\rho(v_2(r))=\begin{cases} \dfrac{(2r/a-1)^{1/2}}{2\pi a^3}=\dfrac{v_2(r)}{2\pi a^3 v_0} \\ 0, \quad r>2a \end{cases} \tag{15}$$

corresponding to using Eq. (8) with $|\psi(v_2(r))|^2$. On the one hand, it seems natural to use $\rho(r)$, since the impact-parameter formulation requires that we work in a coordinate representation. On the other hand, the BEA model itself is developed in velocity space, and the values of total cross sections change if we use $\rho(r)$. Consequently, it is instructive to compare the two approximations.

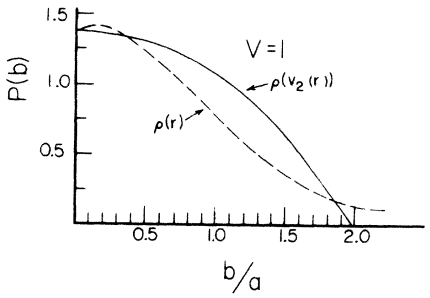

FIG. 2. $P(b)$ vs b at $V=1$. The coordinate-space electron density distribution $\rho(r)$ is given by Eq. (14), and the coordinate representation of the momentum space density distribution $\rho(v_2(r))$, is given by Eqs. (15) and (8). $P(b)$ is the probability per target electron.

In Fig. 2 we have plotted both results near $V=1$. These results are similar, namely, that the shapes are similar (although not identical by any means), and they both give the same values of $b=0$. Furthermore, the two distributions give total cross sections which are within a few percent of each other,[14] except for $V \ll 1$.

In both cases, $P(b)$ may be expressed as

$$P(b) = \int_0^{(R^2-b^2)^{1/2}} \rho^1(r/a) \frac{\sigma(v_i, v_2(r))\, dz}{a^3}, \quad (16)$$

$$\rho^1(r/a) = \begin{cases} e^{-2r/a}, & \rho = \rho(r) \\ (2r/a-1)^{1/2}/2\pi, & \rho = \rho(v_2(r)). \end{cases} \quad (17)$$

In both cases, it is straightforward to show from Eq. (1) that

$$P(b) = (z/Z)^2 f(b/2a, V) \quad (18)$$

where z is the projectile charge, Z is the effective nuclear charge of the target, $a = n^2 a_0/Z$ (n is the principle quantum number of the electron, $a_0 = 5.29\times10^{-9}$ cm) and $V = (mE/MU)^{1/2}$ is the scaled velocity. The effective nuclear charge Z is defined by

$$Z = (|U|/13.6)^{1/2}, \quad (19)$$

where $|U|$ is the binding energy of the target electron. As we shall see later, Eq. (10) will enable us to find $P(b)$ for arbitrary projectiles and targets at various energies from a table of values of $P(b)$ for protons incident on hydrogen.

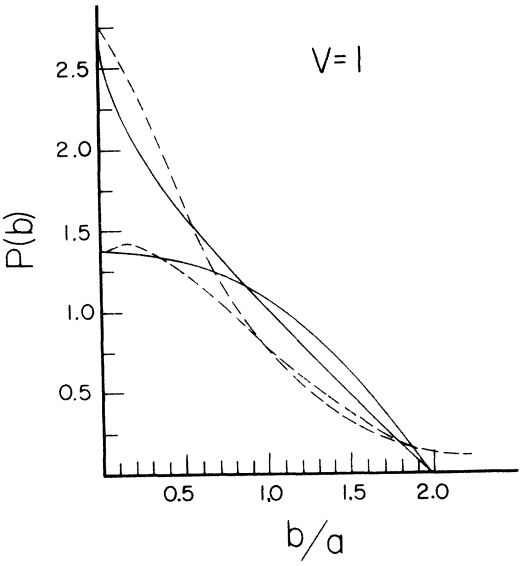

FIG. 3. $P(b)$ vs b at $V=1$. The solid curves are computed using $\rho(r)$, and the dashed curves using $\rho(v_2(r))$. In the upper set of curves, $\sigma(v_i, v_2)$ is assumed to be independent of v_2 in Eq. (12).

TABLE I. $xK_1(x)$ vs x. For $x \gg 1$, $xK_1(x) \to (\pi x/2)^{1/2} e^{-x}$.

x	$xK_1(x)$	x	$xK_1(x)$	x	$xK_1(x)$
0.1	0.985	1.8	0.329	3.5	0.0778
0.2	0.955	1.9	0.303	3.6	0.0713
0.3	0.917	2.0	0.280	3.7	0.0652
0.4	0.874	2.1	0.258	3.8	0.0597
0.5	0.828	2.2	0.237	3.9	0.0546
0.6	0.782	2.3	0.218	4.0	0.0499
0.7	0.735	2.4	0.201	4.1	0.0457
0.8	0.689	2.5	0.185	4.2	0.0417
0.9	0.645	2.6	0.170	4.3	0.0382
1.0	0.602	2.7	0.156	4.4	0.0349
1.1	0.561	2.8	0.143	4.5	0.0319
1.2	0.522	2.9	0.131	4.6	0.0291
1.3	0.484	3.0	0.120	4.7	0.0266
1.4	0.449	3.1	0.110	4.8	0.0243
1.5	0.417	3.2	0.101	4.9	0.0222
1.6	0.385	3.3	0.0928	5.0	0.0202
1.7	0.356	3.4	0.0850		

D. High-Energy Limit

As the speed of the projectile, v_i, becomes much greater than the speed of the target electron, v_2, the scattering cross section given by Eq. (1) becomes independent[3] of v_2. In this high-energy limit, our expression for $P(b)$ takes on a simple form, namely,

$$P(b) = 2\sigma(V) \int_0^{(R^2-b^2)^{1/2}} \rho((b^2+z^2)^{1/2})\, dz, \quad (20)$$

and the expression for $P(0)$ becomes

$$P(0) = \sigma(V) \left\langle \frac{1}{2\pi r^2} \right\rangle. \quad (21)$$

Here $\sigma(V)$ is the total ionization cross section defined by Eq. (3).

The idea of taking $\sigma(v_i, v_2)$ to be independent of v_2 was introduced to Gryzinski[13] several years ago, to estimate ionization probabilities according to

$$P = \sigma(V)/4\pi\bar{r}^2. \quad (22)$$

Gryzinski defined $\bar{r}$ as the mean distance between scattering events, and used it as a parameter in fitting various double ionization data. From Fig. 3 we see that such an approximation is reasonable only at high energies, i.e., $v_i \gg v_0$.

For a hydrogenlike density distribution in coordinate space, corresponding to Eq. (14), the high-energy form of $P(b)$ may be evaluated in closed form; namely,

$$P(b) = \frac{\sigma(V)}{\pi a^2} x K_1(x), \quad (23)$$

where

$x = 2b/a$.

In Table I, $xK_1(x)$ is listed. It is straightforward to show that $P(0) = \sigma(V)/\pi a^2$ for both coordinate and velocity hydrogenic electron density distributions given by Eqs. (14) and (15).

III. CORRESPONDENCE TO SCA

A. Low Energies

In the SCA model when the velocity of the projectile is small compared to the orbit velocity of the target electron, the impact-parameter dependence of $P(b)$ is proportional to an integral over modified Bessel functions; namely,

$$P(b) \sim x^7 \int_x^\infty \left(\frac{K_2(y)}{y^2}\right)^2 dy , \tag{24}$$

where $x = q_0 b$, and q_0 is the minimum momentum transfer of the projectile. Brandt, Jones, and Kraner[6] have pointed out that this may be approximated to a numerical accuracy of ~ 1% by $(a_0 + a_1 x + a_2 x^2)e^{-2x}$, so that $P(b)$ may be expressed at low energies in the SCA model as,

$$P(b) = \frac{\sigma(V)}{(2aV)^2}\,(0.128 + 0.250x + 0.178x^2)\,e^{-2x} . \tag{25}$$

Here we have used $q_0^{-1} = 2aV$, where $a = a_0/Z$ and $V = v_i/v_0$.

Since $\sigma(V) \sim z^2$, we may write Eq. (25) as

$$P(V) = (z/Z)^2 f(b/2a, V) . \tag{26}$$

In other words, the SCA model has the same scaling properties at low energies as the BEA model [cf. Eq. (18)]. It is interesting to note that $P(0)$ may be written in the low-energy SCA model as

$$P(0) = \frac{\sigma(V)}{R^2(V)} , \tag{27}$$

where $R(V)$ is linear in V and a, and $R(V)$ represents the distance at which $P(b)$ tends to zero. At low energies the BEA model qualitatively has the same behavior, as we shall see in Table II.

B. High Energies

In time-dependent perturbation theory, the full scattering wave function is expanded in a basic set of wave functions for the asymptotic Hamiltonian, corresponding to

$$\psi = \sum A_n \phi_n . \tag{28}$$

Substituting these into the Heisenberg equation leads to a set of coupled first-order differential equations for the probability amplitudes, $A_n(t)$. The square of A_n represents the probability that the system is in a state corresponding to ϕ_n, and the cross for scattering into ϕ_n at $t = +\infty$ is given by

$$\sigma_n = \int db\, 2\pi b\, |A_n(\infty)|^2 . \tag{29}$$

In first-order time-dependent perturbation theory for protons in hydrogen, Mittleman[8] has shown that A_n satisfies the following differential equations for excitation to the nth level of hydrogen:

$$\frac{dA_n}{dt} = i \int d^3y\, \phi_n^*(\vec{y})\left(\frac{2}{|\vec{y} - \vec{R}|} + \frac{1}{4}\,\vec{y}\cdot\frac{d^2\vec{R}}{dt^2}\right) \times \phi_i(y)\, e^{i(\epsilon_n - \epsilon_i)} , \tag{30}$$

where $\epsilon_n - \epsilon_i = (E_n - E_i)t$, $\vec{R}$ is the interproton coordinate, and $\vec{y}$ is the electron coordinate relative to the center of mass.

We now apply this to atomic ionization by the impact of fully stripped charged projectiles of charge z. Noting that in the case of ionization there is an additional final-state momentum variable corresponding to the momentum $\vec{k}$ of the electron removed, we write the probability for ionization as

$$P(b) = \int d^3k\, |A_k(b)|^2 . \tag{31}$$

For a straight-line trajectory, corresponding to $\vec{R}(t) = \vec{b} + \vec{v}_i t$, we express A_k as

$$A_k(b) = \int dt\, e^{iW_{ik}t} \int d^3y\, \phi_k^*(\vec{y}) \frac{1}{|\vec{R} - \vec{y}|} \phi_i(\vec{y}) , \tag{32}$$

where $W_{ik} = \frac{1}{2}k^2 - U_i$ (U_i is the binding energy of the hydrogenlike electron in an initial bound state, labeled by i).

Taking the Fourier transform of $|\vec{R} - \vec{y}|^{-1}$, we have

$$A_k(b) = \int dt\, e^{W_{ik}t} \int d^3q\, e^{-i\vec{q}\cdot\vec{R}} \times \int d^3y\, \phi_k^*(\vec{y})\, e^{i\vec{q}\cdot\vec{y}}\, \phi_i(\vec{y}) . \tag{33}$$

In the very-high-energy limit ($v_i \gg v_0$) we may take ϕ_k^* to be a plane wave, and write

$$A_k(b) = \int dt\, e^{iW_{ik}t} \int d^3q\, e^{-i\vec{q}\cdot\vec{R}}\, \Phi_i(\vec{q} - \vec{k}) , \tag{34}$$

where Φ_i is the momentum space wave function of an electron in the ith level of hydrogen.

Using

$$\int d^3q\, e^{-i\vec{q}\cdot\vec{R}}\Phi_i(\vec{q}-\vec{k})$$

$$= e^{-i\vec{k}\cdot\vec{R}}\int d^3q\, e^{i(\vec{k}-\vec{q})\cdot\vec{R}}\Phi_i(\vec{q}-\vec{k})$$

$$= e^{-i\vec{k}\cdot\vec{R}}\,\phi_i^*(\vec{R})\,(2\pi)^3, \qquad (35)$$

where $\phi_i(R)$ is the coordinate wave function, we have

$$A_k(b) = (2\pi)^3\int dt\, e^{iW_{ik}t}\, e^{-i\vec{k}\cdot\vec{R}}\,\phi_i^*(\vec{R}), \qquad (36)$$

whereupon

$$P(b) = (2\pi)^6\iiint dt_1\, dt_2 d^3k\, e^{iW_{ik}(t_1-t_2)} \times e^{-i\vec{k}\cdot\vec{v}_i(t_1-t_2)} \times \phi_i^*(\vec{R}(t_1))\,\phi_i(\vec{R}(t_2)). \qquad (37)$$

For $v_i \gg v_0$, the $e^{iW_{ik}}$ term may be replaced by unity, the $\int d^3k$ is proportional to $v_i^{-1}\,\delta(t_1-t_2)$, and

$$P(b) = \frac{C}{v_i^2}\int dz\,|\phi_i(\vec{R})|^2, \qquad (38)$$

where $z = v_i t$ and $R^2 = b^2 + z^2$. Normalizing to the total ionization cross section, we have for isotropic $\phi_i(R)$,

$$P(b) = \frac{2\sigma(E)}{\pi a^3}\int_0^\infty dz\,\rho(R). \qquad (38)$$

It has been shown that in the high-energy limit, the SCA and BEA models[3,10] give the same value[15] for differential cross sections $d\sigma/dK\,dg$ proportional to E^{-1}. Comparing Eqs. (38) and (23), we see that the SCA and BEA models give the same result for $P(b)/\sigma$ in the same high-energy limit.

This result now solves our dilemma of whether to use $\rho(r)$ or $\rho(v_2(r))$ in the BEA model. According to Eq. (38), $\rho(r)$ is the correct distribution.

Furthermore, we may now use Eq. (23) together with the scaling laws defined by Eq. (18) to predict a universal curve for $P(b)$ at high energies. Our results indicate that the impact-parameter data for all targets and projectiles may be plotted on a single curve as a function of the impact parameter. In Table I we give $xK_1(x)$.

Equations (23) and (38) also indicate that the projectile energy dependence of $P(b)$ is the same as the total ionization cross section $\sigma(V)$ for $V = v_i/v_0 \gg 1$.

IV. RESULTS

A convenient feature of the BEA calculation is that Eq. (18) may be used to scale the results for protons on hydrogen to other targets and projec-

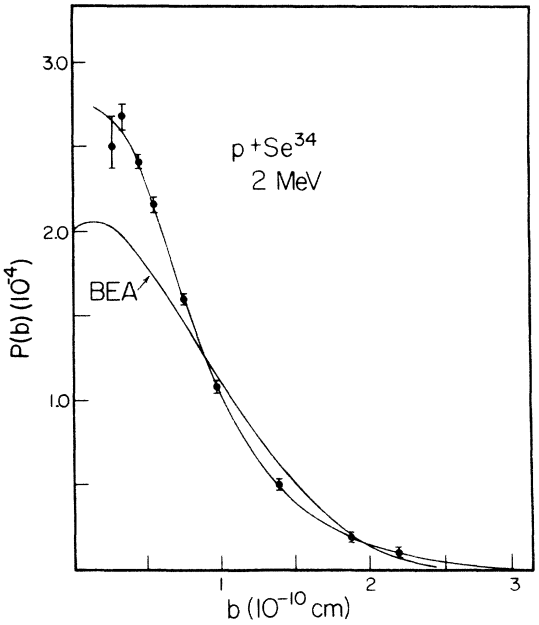

FIG. 4. $p(b)$ vs b for $p + Se^{34}$ at 2 MeV. The upper curve is a fit to the data [Ref. (5)] while the curve labeled BEA corresponds to our calculations. $P(b)$ is the ionization probability per K-shell electron.

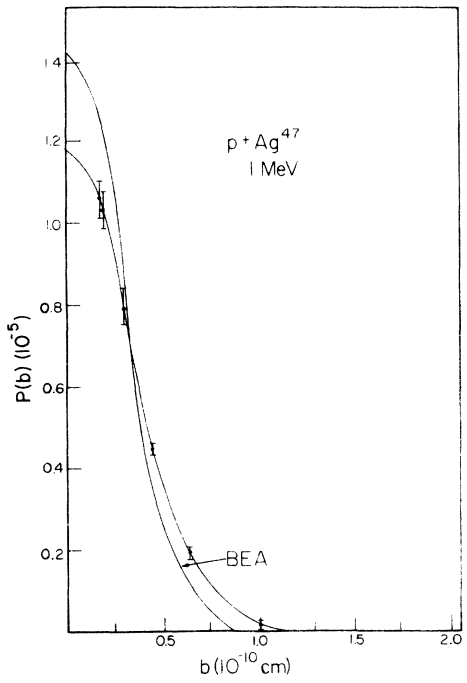

FIG. 5. $P(b)$ vs b for $p + Ag^{47}$ at 1 MeV. The curve representing the data of Ref. (5) has been doubled so that the shapes may be more closely compared; i.e., the theoretical and experimental cross sections differ by about a factor of 2.

TABLE II. $P(b)$ vs b at various V for $z=Z$. Here z is the projectile charge and Z the effective target charge. The impact parameter b is given in units of the radius a of the atomic electron, where $a=a_0/Z$, $a_0=5.29\times10^{-9}$ cm, and $Z=U/13.6$ ($U=\frac{1}{2}mv_0^2$ is the atomic binding energy). The scaled velocity $V=v_i/v_0$ is the ratio of the speed of the projectile divided by v_0. For $z<Z$, $P(b)$ scales as $(z/Z)^2$ at fixed V. To use the table, compute $V=(m_eE_i/M_pU)^{1/2}$, find $P(b)$ from the table, and multiply by $(z/Z)^2$. The coordinate-space hydrogenic K-shell electron density distribution is used.

V \ b	0.05	0.1	0.15	0.2	0.25	0.3	0.35	0.4
0.10	0.642 (−2)	0.517 (−2)	0.303 (−2)	0.123 (−2)	0.222 (−4)			
0.12	0.127 (−1)	0.110 (−1)	0.798 (−2)	0.514 (−2)	0.279 (−2)	0.132 (−2)	0.338 (−3)	
0.14	0.235 (−1)	0.220 (−1)	0.186 (−1)	0.147 (−1)	0.106 (−1)	0.676 (−2)	0.377 (−2)	0.162 (−2)
0.16	0.362 (−1)	0.351 (−1)	0.319 (−1)	0.275 (−1)	0.226 (−1)	0.176 (−1)	0.130 (−1)	0.887 (−2)
0.18	0.510 (−1)	0.503 (−1)	0.471 (−1)	0.425 (−1)	0.369 (−1)	0.311 (−1)	0.253 (−1)	0.200 (−1)
0.20	0.706 (−1)	0.702 (−1)	0.672 (−1)	0.623 (−1)	0.561 (−1)	0.493 (−1)	0.422 (−1)	0.352 (−1)
0.22	0.929 (−1)	0.930 (−1)	0.902 (−1)	0.852 (−1)	0.787 (−1)	0.713 (−1)	0.632 (−1)	0.551 (−1)
0.24	0.117 (0)	0.117 (0)	0.115 (0)	0.110 (0)	0.103 (0)	0.952 (−1)	0.865 (−1)	0.775 (−1)
0.26	0.142 (0)	0.143 (0)	0.141 (0)	0.136 (0)	0.129 (0)	0.121 (0)	0.112 (0)	0.102 (0)
0.28	0.171 (0)	0.173 (0)	0.171 (0)	0.166 (0)	0.158 (0)	0.150 (0)	0.140 (0)	0.129 (0)
0.30	0.202 (0)	0.203 (0)	0.202 (0)	0.197 (0)	0.189 (0)	0.180 (0)	0.170 (0)	0.158 (0)
0.32	0.233 (0)	0.235 (0)	0.234 (0)	0.229 (0)	0.222 (0)	0.212 (0)	0.201 (0)	0.189 (0)
0.34	0.265 (0)	0.268 (0)	0.267 (0)	0.262 (0)	0.255 (0)	0.245 (0)	0.233 (0)	0.221 (0)
0.36	0.298 (0)	0.301 (0)	0.300 (0)	0.295 (0)	0.288 (0)	0.278 (0)	0.266 (0)	0.253 (0)
0.38	0.332 (0)	0.335 (0)	0.335 (0)	0.330 (0)	0.322 (0)	0.312 (0)	0.299 (0)	0.285 (0)
0.40	0.368 (0)	0.371 (0)	0.371 (0)	0.366 (0)	0.358 (0)	0.348 (0)	0.335 (0)	0.320 (0)
0.45	0.460 (0)	0.465 (0)	0.465 (0)	0.461 (0)	0.453 (0)	0.441 (0)	0.427 (0)	0.411 (0)
0.50	0.555 (0)	0.561 (0)	0.562 (0)	0.557 (0)	0.549 (0)	0.537 (0)	0.522 (0)	0.505 (0)
0.60	0.789 (0)	0.797 (0)	0.799 (0)	0.795 (0)	0.785 (0)	0.772 (0)	0.755 (0)	0.736 (0)
0.70	0.979 (0)	0.989 (0)	0.992 (0)	0.988 (0)	0.979 (0)	0.965 (0)	0.946 (0)	0.924 (0)
0.80	0.114 (1)	0.115 (1)	0.115 (1)	0.115 (1)	0.114 (1)	0.112 (1)	0.110 (1)	0.107 (1)
0.90	0.127 (1)	0.128 (1)	0.129 (1)	0.128 (1)	0.127 (1)	0.125 (1)	0.123 (1)	0.120 (1)
1.00	0.139 (1)	0.141 (1)	0.141 (1)	0.141 (1)	0.140 (1)	0.138 (1)	0.135 (1)	0.132 (1)
1.20	0.157 (1)	0.159 (1)	0.159 (1)	0.159 (1)	0.157 (1)	0.155 (1)	0.151 (1)	0.148 (1)
1.40	0.170 (1)	0.172 (1)	0.173 (1)	0.172 (1)	0.171 (1)	0.168 (1)	0.165 (1)	0.160 (1)
1.60	0.179 (1)	0.181 (1)	0.181 (1)	0.180 (1)	0.177 (1)	0.172 (1)	0.167 (1)	0.161 (1)
1.80	0.176 (1)	0.178 (1)	0.179 (1)	0.177 (1)	0.175 (1)	0.170 (1)	0.165 (1)	0.159 (1)
2.00	0.174 (1)	0.177 (1)	0.178 (1)	0.177 (1)	0.174 (1)	0.171 (1)	0.164 (1)	0.152 (1)
2.50	0.177 (1)	0.177 (1)	0.172 (1)	0.164 (1)	0.154 (1)	0.143 (1)	0.124 (1)	0.108 (1)
3.00	0.145 (1)	0.146 (1)	0.144 (1)	0.138 (1)	0.120 (1)	0.102 (1)	0.878 (0)	0.760 (0)
3.50	0.125 (1)	0.128 (1)	0.127 (1)	0.105 (1)	0.886 (0)	0.754 (0)	0.648 (0)	0.561 (0)
4.00	0.114 (1)	0.120 (1)	0.989 (0)	0.810 (0)	0.680 (0)	0.579 (0)	0.498 (0)	0.431 (0)
5.00	0.107 (1)	0.811 (0)	0.635 (0)	0.520 (0)	0.436 (0)	0.372 (0)	0.320 (0)	0.277 (0)
6.00	0.765 (0)	0.564 (0)	0.442 (0)	0.362 (0)	0.303 (0)	0.258 (0)	0.222 (0)	0.192 (0)
7.00	0.562 (0)	0.414 (0)	0.325 (0)	0.266 (0)	0.223 (0)	0.190 (0)	0.163 (0)	0.142 (0)
8.00	0.431 (0)	0.317 (0)	0.249 (0)	0.204 (0)	0.171 (0)	0.146 (0)	0.125 (0)	0.108 (0)
9.00	0.340 (0)	0.251 (0)	0.197 (0)	0.161 (0)	0.135 (0)	0.115 (0)	0.989 (−1)	0.857 (−1)
10.00	0.276 (0)	0.203 (0)	0.159 (0)	0.130 (0)	0.109 (0)	0.932 (−1)	0.801 (−1)	0.694 (−1)

V \ b	0.45	0.5	0.6	0.7	0.8	0.9	1.0	1.1
0.10								
0.12								
0.14	0.582 (−3)	0.553 (−4)						
0.16	0.550 (−2)	0.287 (−2)	0.269 (−3)					
0.18	0.151 (−1)	0.108 (−1)	0.430 (−2)	0.795 (−3)	0.343 (−5)			
0.20	0.286 (−1)	0.225 (−1)	0.126 (−1)	0.579 (−2)	0.166 (−2)	0.832 (−4)		
0.22	0.471 (−1)	0.394 (−1)	0.256 (−1)	0.147 (−1)	0.714 (−2)	0.262 (−2)	0.356 (−3)	
0.24	0.685 (−1)	0.596 (−1)	0.429 (−1)	0.286 (−1)	0.171 (−1)	0.867 (−2)	0.353 (−2)	0.785 (−3)
0.26	0.916 (−1)	0.816 (−1)	0.626 (−1)	0.455 (−1)	0.309 (−1)	0.191 (−1)	0.102 (−1)	0.433 (−2)
0.28	0.118 (0)	0.107 (0)	0.846 (−1)	0.646 (−1)	0.472 (−1)	0.326 (−1)	0.207 (−1)	0.115 (−1)
0.30	0.146 (0)	0.134 (0)	0.120 (0)	0.867 (−1)	0.660 (−1)	0.482 (−1)	0.336 (−1)	0.217 (−1)

TABLE II *(Continued)*

V \ b	0.45	0.5	0.6	0.7	0.8	0.9	1.0	1.1
0.32	0.176 (0)	0.163 (0)	0.137 (0)	0.111 (0)	0.877 (−1)	0.668 (−1)	0.487 (−1)	0.340 (−1)
0.34	0.207 (0)	0.193 (0)	0.165 (0)	0.137 (0)	0.111 (0)	0.877 (−1)	0.667 (−1)	0.486 (−1)
0.36	0.239 (0)	0.224 (0)	0.194 (0)	0.164 (0)	0.136 (0)	0.110 (0)	0.867 (−1)	0.658 (−1)
0.38	0.271 (0)	0.255 (0)	0.223 (0)	0.192 (0)	0.162 (0)	0.134 (0)	0.108 (0)	0.848 (−1)
0.40	0.304 (0)	0.288 (0)	0.253 (0)	0.220 (0)	0.188 (0)	0.158 (0)	0.130 (0)	0.105 (−1)
0.45	0.394 (0)	0.375 (0)	0.336 (0)	0.296 (0)	0.256 (0)	0.219 (0)	0.187 (0)	0.158 (0)
0.50	0.486 (0)	0.466 (0)	0.424 (0)	0.380 (0)	0.336(0)	0.290 (0)	0.245 (0)	0.212 (0)
0.60	0.714 (0)	0.691 (0)	0.642 (0)	0.593 (0)	0.546 (0)	0.501 (0)	0.453 (0)	0.406 (0)
0.70	0.900 (0)	0.873 (0)	0.816 (0)	0.755 (0)	0.694 (0)	0.635 (0)	0.577 (0)	0.523 (0)
0.80	0.104 (1)	0.101 (1)	0.947 (0)	0.877 (0)	0.807 (0)	0.739 (0)	0.676 (0)	0.616 (0)
0.90	0.117 (1)	0.113 (1)	0.106 (1)	0.984 (0)	0.907 (0)	0.828 (0)	0.750 (0)	0.676 (0)
1.00	0.129 (1)	0.125 (1)	0.116 (1)	0.107 (1)	0.976 (0)	0.884 (0)	0.798 (0)	0.717 (0)
1.20	0.143 (1)	0.139 (1)	0.128 (1)	0.118 (1)	0.106 (1)	0.941 (0)	0.821 (0)	0.690 (0)
1.40	0.155 (1)	0.148 (1)	0.134 (1)	0.119 (1)	0.104 (1)	0.860 (0)	0.697 (0)	0.562 (0)
1.60	0.154 (1)	0.147 (1)	0.131 (1)	0.110 (1)	0.882 (0)	0.704 (0)	0.563 (0)	0.451 (0)
1.80	0.152 (1)	0.142 (1)	0.116 (1)	0.915 (0)	0.723 (0)	0.574 (0)	0.457 (0)	0.365 (0)
2.00	0.139 (1)	0.124 (1)	0.968 (0)	0.758 (0)	0.597 (0)	0.473 (0)	0.376 (0)	0.301 (0)
2.50	0.942 (0)	0.824 (0)	0.637 (0)	0.497 (0)	0.391 (0)	0.310 (0)	0.246 (0)	0.197 (0)
3.00	0.662 (0)	0.579 (0)	0.447 (0)	0.349 (0)	0.275 (0)	0.217 (0)	0.173 (0)	0.138 (0)
3.50	0.489 (0)	0.427 (0)	0.330 (0)	0.258 (0)	0.203 (0)	0.161 (0)	0.128 (0)	0.102 (0)
4.00	0.375 (0)	0.328 (0)	0.254 (0)	0.198 (0)	0.156 (0)	0.123 (0)	0.982 (−1)	0.785 (−1)
5.00	0.241 (0)	0.211 (0)	0.163 (0)	0.127 (0)	0.100 (0)	0.793 (−1)	0.631 (−1)	0.505 (−1)
6.00	0.168 (0)	0.147 (0)	0.113 (0)	0.885 (−1)	0.697 (−1)	0.552 (−1)	0.439 (−1)	0.351 (−1)
7.00	0.123 (0)	0.108 (0)	0.833 (−1)	0.651 (−1)	0.512 (−1)	0.406 (−1)	0.323 (−1)	0.258 (−1)
8.00	0.944 (−1)	0.826 (−1)	0.638 (−1)	0.499 (−1)	0.393 (−1)	0.311 (−1)	0.248 (−1)	0.198 (−1)
9.00	0.746 (−1)	0.653 (−1)	0.505 (−1)	0.394 (−1)	0.310 (−1)	0.246 (−1)	0.196 (−1)	0.157 (−1)
10.00	0.604 (−1)	0.529 (−1)	0.409 (−1)	0.319 (−1)	0.251 (−1)	0.199 (−1)	0.159 (−1)	0.127 (−1)

V \ b	1.2	1.3	1.4	1.5	1.6	1.7	1.8	1.9
0.10								
0.12								
0.14								
0.16								
0.18								
0.20								
0.22								
0.24	0.372 (−5)							
0.26	0.124 (−2)	0.379 (−4)						
0.28	0.513 (−2)	0.161 (−2)	0.105 (−3)					
0.30	0.124 (−1)	0.569 (−2)	0.182 (−2)	0.150 (−3)				
0.32	0.222 (−1)	0.129 (−1)	0.592 (−2)	0.185 (−2)	0.121 (−3)			
0.34	0.338 (−1)	0.222 (−1)	0.128 (−1)	0.574 (−2)	0.165 (−2)	0.427 (−4)		
0.36	0.478 (−1)	0.330 (−1)	0.216 (−1)	0.122 (−1)	0.503 (−2)	0.120 (−2)		
0.38	0.642 (−1)	0.462 (−1)	0.318 (−1)	0.205 (−1)	0.106 (−1)	0.389 (−2)	0.478 (−3)	
0.40	0.822 (−1)	0.617 (−1)	0.438 (−1)	0.301 (−1)	0.189 (−1)	0.928 (−2)	0.256 (−2)	0.944 (−6)
0.45	0.131 (0)	0.107 (0)	0.836 (−1)	0.614 (−1)	0.436 (−1)	0.302 (−1)	0.161 (−1)	0.513 (−2)
0.50	0.183 (0)	0.155 (0)	0.130 (0)	0.106 (0)	0.728 (−1)	0.576 (−1)	0.429 (−1)	0.187 (−1)
0.60	0.363 (0)	0.325 (0)	0.291 (0)	0.267 (0)	0.246 (0)	0.218 (0)	0.199 (0)	0.185 (0)
0.70	0.475 (0)	0.433 (0)	0.395 (0)	0.357 (0)	0.323 (0)	0.294 (0)	0.265 (0)	0.231 (0)
0.80	0.558 (0)	0.503 (0)	0.452 (0)	0.406 (0)	0.361 (0)	0.314 (0)	0.267 (0)	0.224 (0)
0.90	0.607 (0)	0.544 (0)	0.480 (0)	0.416 (0)	0.351 (0)	0.293 (0)	0.244 (0)	0.202 (0)
1.00	0.633 (0)	0.551 (0)	0.465 (0)	0.386 (0)	0.318 (0)	0.262 (0)	0.216 (0)	0.178 (0)
1.20	0.567 (0)	0.462 (0)	0.376 (0)	0.306 (0)	0.249 (0)	0.203 (0)	0.166 (0)	0.136 (0)
1.40	0.453 (0)	0.366 (0)	0.295 (0)	0.239 (0)	0.194 (0)	0.158 (0)	0.129 (0)	0.106 (0)

TABLE II *(Continued)*

V \ b	1.2	1.3	1.4	1.5	1.6	1.7	1.8	1.9
1.60	0.362 (0)	0.291 (0)	0.235 (0)	0.190 (0)	0.154 (0)	0.125 (0)	0.102 (0)	0.837 (−1)
1.80	0.293 (0)	0.236 (0)	0.190 (0)	0.153 (0)	0.124 (0)	0.101 (0)	0.826 (−1)	0.677 (−1)
2.00	0.241 (0)	0.194 (0)	0.156 (0)	0.126 (0)	0.102 (0)	0.833 (−1)	0.679 (−1)	0.557 (−1)
2.50	0.158 (0)	0.127 (0)	0.102 (0)	0.826 (−1)	0.669 (−1)	0.545 (−1)	0.445 (−1)	0.365 (−1)
3.00	0.111 (0)	0.891 (−1)	0.718 (−1)	0.581 (−1)	0.470 (−1)	0.383 (−1)	0.313 (−1)	0.257 (−1)
3.50	0.819 (−1)	0.659 (−1)	0.531 (−1)	0.430 (−1)	0.348 (−1)	0.284 (−1)	0.232 (−1)	0.190 (−1)
4.00	0.630 (−1)	0.507 (−1)	0.409 (−1)	0.330 (−1)	0.268 (−1)	0.218 (−1)	0.178 (−1)	0.146 (−1)
5.00	0.405 (−1)	0.326 (−1)	0.263 (−1)	0.213 (−1)	0.172 (−1)	0.140 (−1)	0.115 (−1)	0.940 (−2)
6.00	0.282 (−1)	0.227 (−1)	0.183 (−1)	0.148 (−1)	0.120 (−1)	0.978 (−2)	0.799 (−2)	0.655 (−2)
7.00	0.207 (−1)	0.167 (−1)	0.135 (−1)	0.109 (−1)	0.883 (−2)	0.720 (−2)	0.588 (−2)	0.482 (−2)
8.00	0.159 (−1)	0.128 (−1)	0.103 (−1)	0.835 (−2)	0.677 (−2)	0.552 (−2)	0.451 (−2)	0.370 (−2)
9.00	0.126 (−1)	0.101 (−1)	0.816 (−2)	0.660 (−2)	0.535 (−2)	0.436 (−2)	0.356 (−2)	0.292 (−2)
10.00	0.102 (−1)	0.820 (−2)	0.661 (−2)	0.535 (−2)	0.434 (−2)	0.354 (−2)	0.289 (−2)	0.237 (−2)

tiles. In Table II we present values of $P(b)$ as a function of b over a range of scaled velocities V. At large scaled velocities, we see that the shape of $P(b)$ tends to be independent of V, and at low scaled velocities we see that the cutoff distance is roughly linear in V, both in accord with earlier discussion.

In Figs. 4–6 we compare our results to the experimental data of Laegsgaard, Andersen, and Feldman,[5] as well as to SCA results[10] taken from their paper. In general, the shapes of $P(b)$ are in somewhat better agreement than the total cross sections. The BEA values of $P(b)$ tend to come into $b=0$ with zero slope, while the SCA values of $P(b)$ have a finite slope near $b=0$. Compared to experiment, the BEA calculations tend to cut off too quickly, while the SCA results tend to overshoot at large impact parameters. For 2 MeV $p+Ag^{47}$, the low-energy SCA result given Brandt, Jones, and Kraner[6] (not shown) is within 35% of the full SCA calculation at all values of b. In this case $V=0.206$.

In Fig. 7 we compare BEA, full SCA, low-energy SCA, and experiment for 2-MeV protons on copper. The comparisons of BEA, SCA, and experiment are not dissimilar from those given above, except that in this case the BEA result has a shape somewhat closer to experiment than the SCA result. The full and low-energy SCA results are

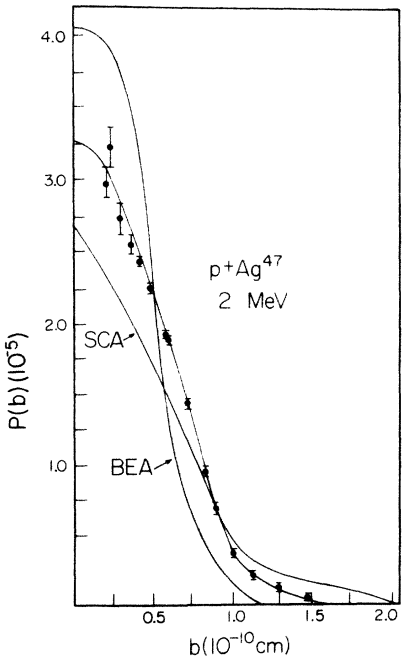

FIG. 6. $P(b)$ vs b for $p+Ag^{47}$ at 2 MeV. The curve labeled SCA corresponds to the calculations of Ref. 10.

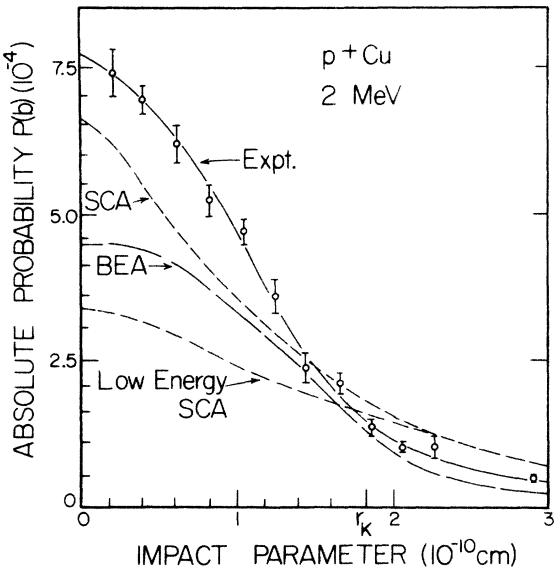

FIG. 7. $P(b)$ vs b for $p+Cu^{29}$ at 2 MeV. The low-energy SCA curve corresponds to Ref. 6.

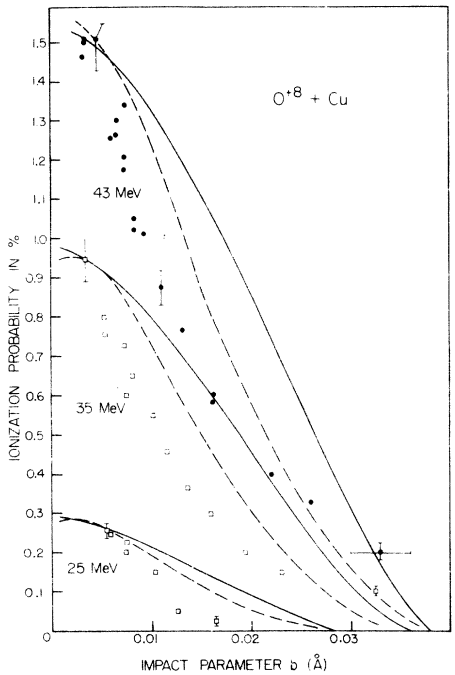

FIG. 8. $P(b)$ vs b for O^{+8} + Cu at 25, 35, and 43 MeV. The theoretical curves have been normalized to the data points [Ref. (7)] near $b=0$. Experimental and theoretical total cross sections differ by a factor of from 3 to 6. In this case, the dashed curves represent BEA calculations using $\rho(r)$ and the solid curves represent BEA calculations using $\rho(v_2(r))$.

within 10% for $b \gtrsim r_K$,[16] but at $b=0$ the full SCA calculation is twice the low-velocity result. In this case the scaled velocity V is 0.35 (corresponding to a value of $\xi_K \cong 0.8$ in the notation of Brandt, Jones, and Kraner). However, the total cross sections are within 10%, since $\int db\, 2\pi b P(b)$ tends to suppress the values of $P(b)$ near $b=0$.

In Fig. 8 we compare the shapes of the BEA predictions to recent results of Cocke[7] for $O+Cu$ at 25, 35, and 43 MeV. The predicted values of $P(0)$ are 3 to 6 times larger than experiment, and we have normalized to a point near $b=0$. The shapes for coordinate-space density target-electron distributions are favored over the velocity space distribution, in accord with Sec. III. The SCA calculation (not shown) lies within experimental error at most values of b when normalized to the experimental cross section in this case.

V. DISCUSSION

In the BEA and SCA calculations, the probability for ionization is much smaller than unity and of similar magnitude when the projectile charge z is small compared to the effective nuclear charge Z. This is consistent with perturbation theory upon which the SCA, and presumably the BEA, calculations are based. However, since both scale as z^2, as z/Z increases the ionization probability increases, and for $z \sim Z$, $P(b)$ exceeds unity near $V=1$, throwing into serious doubt the validity of either the BEA or SCA calculation. One temporary remedy is to argue, at least at low scaled velocities, increased binding-energy effects become more important as z/Z increases, and that the unperturbed nuclear charge Z must be replaced by an increased charge $(Z+\epsilon z)$, where ϵ is an energy-dependent parameter such as that of Brandt, Basbas, and Laubert.[17] Another remedy is to use Hansen's constrained probability, which can never exceed unity. However, since perturbation theory, itself, is of questionable application, it seems more appropriate to adopt a completely different approach, such as that of Russek[18] where energy lost by the projectile is statistically distributed among the electrons of the target atom.

It is not proper, from a quantum-mechanical point of view, to use an algebraic one-to-one relationship between the position and velocity of the orbiting atomic electron as in Eq. (8). Rather the relationship should be statistical, so that at each value of r there is a range of values of v_2 in accord with the uncertainty principle. Such a statistical spread means that for $r > 2a$ in Eq. (8), it will be possible to have well-defined nonzero values of v_2. Consequently, $P(b)$ will tend to spread out toward larger impact parameters when quantum mechanics is introduced. Relaxing the peaking approximation introduced in Sec. II B will also tend to spread out the probability distribution. In the SCA calculations the Hamiltonian of the atomic electron is treated quantum mechanically, giving rise to relatively larger values of $P(b)$ at large impact parameters.

In Sec. IV we remarked that there is better agreement on the shape of $P(b)$, in comparing to existing data, than on the normalization. However, the importance of the shape of $P(b)$ should not be minimized for it contributes to calculations of multiple ionization phenomena where combinations of $P(b)$ are used. For example, double K-shell ionization is proportional to $\int db\, 2\pi b \times [P(b)]^2$, for $P(b) \ll 1$. Normalizing both results to the same single ionization cross section, we find a factor-of-3 difference between low-energy SCA calculations and BEA calculations[19] of double K-shell ionization for 30-MeV O^{+6} + Ca, where $V=0.5$. The factor of 3 is entirely due to differences in the shape of $P(b)$.

At low energies ($V \ll 1$) in the SCA approximation, $bP(b)$ peaks when $q_0 b \cong 1.05$. Since $q_0 = 1/(2aV)$, $V \ll \frac{1}{2}$ implies that $q_0^{-1} \ll a$, where a is

the radius of the participating electron. In other words, as we have noted, at low velocities, the cutoff distance for $P(b)$ is determined by q_0^{-1}, which is linear in V in the SCA calculations. From Table II we see that the BEA and SCA calculations are qualitatively similar at low V. As V approaches unity in our BEA calculations, the cutoff distance saturates near $2a$, and the shape of $P(b)$ changes from a characteristic low-energy shape to the universal high-energy shape given by Eq. (23). At high velocities the cutoff distance remains fixed near $2a$. The maximum of $P(b)$ occurs near $V \cong 1.5$, while the cross section maximizes near $V \cong 1.0$ in the BEA model.

Recently, Wu, Hill, and Merzbacher[20] have computed the effects of excitation to the first excited level of electrons found in an isotropic harmonic oscillator, and found that much of the contribution to $P(b)$ occurs at impact parameters greater than $2a$. Interpreting this as a projectile-induced distortion of the atom which has been included in neither our calculation nor the SCA calculations, suggests motivation for careful study of $P(b)$ at large impact parameters. At small impact parameters, there has been some recent experimental evidence[21] of a dramatic increase of $P(b)$ possibly due to molecular-orbital effects at low energies.

Computing $P(b)$ in the BEA model is relatively simple. Using Eqs. (1) and (16), one integral is done numerically. Forty values of $P(b)$ may be thus computed in about 30 sec on a relatively slow IBM 360/50. In contrast, the full SCA calculation requires the equivalent of four numerical integrations corresponding to a double integration over a product of a Bessel function and a hypergeometric function.

Another advantage of the BEA calculation of $P(b)$ is that it may be trivially extended to other systems. By adjusting the range of energy transfers over which one integrates, one may evaluate $P(b)$ for excitation. Furthermore, one could use the procedure to evaluate $P(b)$ for atomic ionization and excitation by electron impact. However, in all of these extensions, one should check his theoretical footing before proceeding with numerical calculations.

ACKNOWLEDGMENTS

I am indebted to C. P. Bhalla, D. Burch, C. L. Cocke, J. D. Garcia, J. S. Hansen, E. Merzbacher, P. Richard, and L. Weaver for helpful discussions. I also thank M. Klug and G. Strand for assistance with the calculations.

[1] E. Merzbacher, in *Proceedings of the International Conference on Inner Shell Ionization Phenomena, Atlanta, Georgia, 1972,* edited by R. W. Fink *et al.* (U.S. Atomic Energy Commission, Oak Ridge, Tenn., 1973); G. S. Kendelwal, B. H. Choi, and E. Merzbacher, Data 1, 103 (1969); E. Merzbacher and W. H. Lewis, *Handbuch der Physik* (Springer-Verlag, Berlin, 1958), Vol. 34, p. 166.

[2] E. Gerjuoy, Phys. Rev. 148, 54 (1966); L. Vriens, Proc. Phys. Soc. Lond. 90, 935 (1966); J. D. Garcia, E. Gerjuoy, and J. Wekler, Phys. Rev. 165, 66 (1968), J. D. Garcia, Phys. Rev. A 4, 955 (1971); J. D. Garcia, Phys. Rev. A 1, 280 (1970).

[3] J. D. Garcia, Phys. Rev. 159, 39 (1967).

[4] H. J. Stein, H. O. Lutz, P. H. Mokler, K. Sistemich, and P. Ambruster, Phys. Rev. Lett. 24, 701 (1970); Phys. Rev. A 2, 2575 (1970); and Phys. Rev. A 5, 2126 (1972).

[5] E. Laegsgaard, J. V. Andersen, and L. C. Feldman, in *Proceedings of the International Conference on Inner Shell Ionization Phenomena, Atlanta, Georgia, 1972,* edited by R. W. Fink *et al.* (U.S. Atomic Energy Commission, Oak Ridge, Tenn., 1973); Phys. Rev. Lett. 29, 1206 (1973).

[6] W. Brandt, K. W. Jones, and H. W. Kraner, Phys. Rev. Lett. 30, 351 (1973).

[7] C. L. Cocke and R. Randall, Phys. Rev. Lett. 30, 1016 (1973).

[8] M. H. Mittleman, Phys. Rev. 122, 499 (1961).

[9] J. Bang and J. M. Hansteen, K. Dan. Vidensk. Selsk. Mat. Fys. Medd. 31, No. 12 (1959).

[10] J. M. Hansteen and O. P. Mosebekk, Z. Phys. 234, No. 13 (1970); J. M. Hansteen and O. P. Mosebekk (unpublished).

[11] The factor of $|\vec{v}_i - \vec{v}_2|4\pi$ in Eqs. (1), (4), and (9) is necessary to avoid infinite Coulomb cross sections. Further details may be found in Refs. 2 and 13.

[12] J. H. McGuire and P. Richard, Phys. Rev. A 8, 1374 (1973).

[13] M. Gryzinski, Phys. Rev. 138, A336 (1965).

[14] J. S. Hansen, private communication; Phys. Rev. A 8, 822 (1973).

[15] D. R. Bates and W. R. McDonaugh, J. Phys. B 5, L107 (1972); J. Phys. B 3, L83 (1970). It is worth emphasizing that the equality between BEA and SCA is also derived by replacing the Coulomb wave function between the target and ejected electron by a plane wave. However, the $\ln E/E$ term in the total cross section is missing in the BEA result, so that at very high energies the BEA and full SCA cross sections are quite different.

[16] There is not a large difference between $r_K \equiv a_0/Z_{\text{nucl}}$ and $a \equiv a_0/Z$, where $a_0 = 5.3 \times 10^{-9}$ cm, Z_{nucl} is the charge of the target nucleus, and Z is given by Eq. (19).

[17] W. Brandt, G. Basbas, and R. Laubert, Phys. Rev. A 7, 983 (1973).

[18] A. Russek, Phys. Rev. 132, 246 (1963); A. Russek and J. Meli, Physica 46, 222 (1970).

[19] J. H. McGuire, Phys. Rev. A (to be published).

[20] J. Wu, K. W. Hill, and E. Merzbacher, Bull. Am. Phys. Soc. 18, 662 (1973).

[21] C. L. Cocke (private communication).

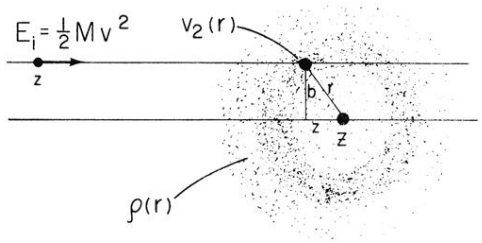

FIG. 1. Representation of the BEA Model. The incident projectile with velocity v_i scatters via a two-body Coulomb interaction from an electron with velocity v_2. The atomic electron is characterized by a density distribution $\rho(r)$.